Primary Amphipathic Cell-Penetrating Peptides: Structural Requirements and Interactions with Model Membranes†

Sébastien Deshayes,‡ Thomas Plénat,§ Gudrun Aldrian-Herrada,‡ Gilles Divita,‡ Christian Le Grimellec,§ and Frédéric Heitz*,‡

CRBM, CNRS-FRE 2593, 34293 Montpellier Cedex 5, France, and CBS, INSERM-U 554, 34090 Montpellier Cedex 5, France

Received April 8, 2004; Revised Manuscript Received April 29, 2004

ABSTRACT: To identify rules for the design of efficient cell-penetrating peptides that deliver therapeutic agents into subcellular compartments, we compared the properties of two closely related primary amphipathic peptides that mainly differ by their conformational state. On the basis of a peptide Pβ that is nonstructured in water and that promotes efficient cellular uptake of nucleic acids through noncovalent association, we have designed a peptide [Pα] that is predicted to adopt a helical conformation. We show that [Pβ] undergoes a lipid-induced conformational transition into a sheet structure, while [Pα] remains helical. Penetration experiments show that both peptides can spontaneously insert into phospholipid membranes. Analysis of compression isotherms indicates that both peptides interact with phospholipids in the liquid expanded and liquid condensed states. AFM observations reveal that the peptides strongly disrupt the lipid organization of the monolayers and that the conformational state can influence the uptake by model membranes.

Over the past 10 years, substantial progress has been made in the development of peptide-based systems that facilitate intracellular delivery of drugs and/or nucleic acids (*1*−*7*). However, in most cases, the efficiency of delivery remains unsatisfactory, mainly due to sensitivity to medium and/or cytotoxicity of the vectors (*8*−*10*). With the aim of increasing the potency of cellular internalization of such vectors, we designed two new peptides. Two main criteria, differing from those previously reported (*1*−*7*, *11*−*15*), were chosen for this design: (*i*) the peptide must contain a hydrophobic sequence for membrane binding; (*ii*) the vector must contain a hydrophilic sequence bearing a signal targeting a subcellular compartment. We selected a nuclear localization sequence (NLS)[1] (*16*) that has the advantage of being highly hydrophilic and thus improving water solubilization of the peptide. A second advantage of this latter sequence lies in the presence of positively charged residues that can favor interactions with nucleic acids. In particular, we chose the NLS of SV40 large T antigen (*17*, *18*). With respect to the hydrophobic sequences, we selected the signal peptide (SP) of the Ig(V) light chain of *caiman crocodylus* (*19*) on one hand and a derivative of the fusion sequence (FP) of HIV1 gp41 protein (*20*) on the other. The hydrophobic and hydrophilic sequences were linked through the W-S-Q spacer to improve flexibility and to retain the integrity of the two sequences. Both peptides, SP−NLS and FP−NLS, respectively, are acetylated at their N-terminus and bear a cysteamide group at their C-terminal. They were both shown to be rapidly internalized in cells and to localize mainly to the nucleus (*2*, *17*, *18*, *21*). Previous investigations related to the elucidation of the mechanism involved in the membrane translocation process revealed puzzling behaviors when comparing both peptides. Although both show almost the same conformational behavior when in solution (nonstructured in water and partly α-helical in the presence of TFE) or in the presence of SDS micelles (α-helical in the hydrophobic domain) (*17*, *22*), their ability to adsorb at air−water interfaces and to penetrate into phospholipid monolayers is strongly sequence-dependent. Indeed, a preliminary study of the penetration of both these peptides into phospholipid monolayers showed that the variations of surface pressure induced by the former peptide does not depend on the nature of the lipid headgroups, while in the case of the second peptide, penetration into neutral phospholipids is poor. To understand and identify the criteria that define an efficient membrane penetrating peptide and a good agent for intracellular delivery, we undertook investigations on two closely related peptides derived from the FP−NLS peptide. Here, we describe the influence of modifications of the hydrophobic sequence on the conformational properties of the amphipathic peptide together with the effect on the ability of the modified peptides to penetrate into various types of model membranes. These will be discussed in connection with the transfection potency of these peptides.

MATERIALS AND METHODS

Peptides. All peptides were synthesized by solid-phase peptide synthesis using aminoethyldithio 2-isobutyric acid-Expansin resin on a Pioneer Peptide Synthesizer (Applied

† This work was supported by EU grant QLK2-CT-2001-01451.

* To whom correspondence should be addressed. CRBM, CNRS−FRE 2593, 1919, route de Mende, 34293 Montpellier Cedex 5, France. Tel.: + 33 (0)4 67 61 33 92. Fax: + 33 (0)4 67 52 15 59. E-mail: heitz@crbm.cnrs-mop.fr.

‡ CRBM.

§ CBS.

[1] Abbreviations: AFM, atomic force microscopy; NLS, nuclear localization sequence; SP, signal peptide; FP, fusion peptide; DOPC, dioleoylphosphatidylcholine; DOPG, dioleoylphosphatidylglycerol: DPPC, dipalmitoylphosphatidylcholine; DPPG, dipalmitoylphosphatidylglycerol; CPI, critical pressure of insertion; LE, liquid expanded; LC, liquid condensed.

10.1021/bi049298m CCC: $27.50
Published on Web 05/22/2004

Table 1: Identification of the Two Peptides (Elution and Molecular Weights) and Their Critical Pressures of Insertion (CPI) into Various Phospholipids[a]

peptide	[Pβ]	[Pα]
elutions	43.5%	62%
Mw (theor)	2908.6	3046.9
Mw (exp: MH+)	2906	3044
DOPC	33	33
DOPG	48	39
DPPC	30	37
DPPG	38	37

[a] The elution profiles are related to the percentage of acetonitrile in the acetontrile/TFA 0.1% gradient at a flow rate of 5 mL/min. For the determination of the CPI, the peptide concentrations were 0.25 and 0.375 μM for [Pβ] and [Pα], respectively.

Biosystems, Foster City, CA) according to the Fmoc/tBu method, as already described (*23*). The peptides that have the following sequences: G−A−L−F−L−G−F−L−G−A^{10}−A−G−S−T−M−G−A−W−S−Q^{20}−P−K−K−K−R−K−V and G−A−L−F−L−A−F−L−A−A^{10}−A−L−S−L−M−G−L−W−S−Q^{20}−P−K−K−K−R−K−V for [Pβ] and [Pα], respectively, were acetylated at their N-terminus. Owing to the nature of the modification of the resin, both peptides bear a cysteamide group (−NH−CH_2−CH_2−SH) at their C-terminus. Double couplings were performed at crucial steps, namely at residues V^{27}, R^{25}, K^{24}, S^{19}, and T^{14} for [Pβ] and R^{25}, K^{24}, S^{19} and L^{14} for [Pα]. After side chain deprotection, the crude peptides (yields 95 and 92% for [Pβ] and [Pα], respectively) were purified by semipreparative HPLC, leading to peptides containing less than 1% impurity as assessed by analytical HPLC. Mass spectra analysis and HPLC characteristics are reported in Table 1.

Phospholipids. Dioleoylphosphatidylcholine (DOPC), dioleoylphosphatidylglycerol (DOPG), dipalmitoylphosphatidylcholine (DPPC), and dipalmitoylphosphatidylglycerol (DPPG) were purchased from Avanti Polar Lipids (Alabaster, AL).

Fourier Transform Infra-Red (FTIR) Spectroscopy. FTIR spectra were obtained on a Bruker (Wissembourg, France) IFS 28 spectrometer equipped with a liquid nitrogen cooled MCT detector. Spectra (1000−2000 scans) were recorded at a spectral resolution of 4 cm^{-1} and were analyzed using the OPUS/IR2 program. Samples were obtained by deposition of solutions of lipid and peptide mixtures onto a fluorine plate, where the solvents were allowed to evaporate under a nitrogen flux.

Circular Dichroism (CD) Measurements. CD spectra were recorded on a Jasco 810 (Tokyo, Japan) dichrograph in a quartz cell with an optical path of 1 mm for peptide in aqueous solutions. For samples transferred by the Langmuir−Blodgett (LB) method (see below), quartz plates were used, and eight plates were gathered to amplify the detected signal (*24*). The band positions were determined after smoothing the spectra by applying the method of Savitzky−Golay.

Adsorption at the Air−Water Interface. Adsorption studies at the air−water interface were carried out using a microtrough S and analyzed with the Film Ware 2.41 program from Kibron, Inc. (Helsinki, Finland). Measurements were made at equilibrium after injection of aliquots of an aqueous solution of peptide into the aqueous subphase and gentle stirring with a magnetic stirrer. To determine the Critical Micellar Concentration (CMC), this procedure was repeated until no further increase in surface pressure could be detected.

For penetration measurements of peptides into phospholipids, a lipid monolayer was initially prepared by spreading a solution of lipid in chloroform/methanol (3/1, v/v) onto the air/NaCl aqueous solution interface to obtain a defined surface pressure. The solvent was allowed to evaporate, and when a constant surface pressure was reached, a small volume of the aqueous peptide solution was injected into the subphase beneath the lipid monolayer. Increases in surface pressure were recorded for different initial lipid surface pressures to determine the critical pressure of insertion (CPI) of peptides into the lipid.

Langmuir−Blodgett Monolayers. All transfers onto quartz slides or mica were achieved using a homemade setup with a procedure described previously (*25*). During LB transfers, the surface pressure was maintained constant through a feedback system and was chosen to be close to that of the collapse pressure of pure peptides.

Compression isotherms of monolayers were recorded using a Langmuir balance setup with a 657-cm^2 trough. Surface tensions were measured with a Prolabo (Paris, France) tensiometer, by the platinum plate method of Wilhelmy. Isotherms were recorded on a XY Kipp and Zonen (Delft, The Netherlands) model BD 91 recorder. DPPC, DPPG, DOPC, and DOPG solutions were prepared by dissolving phospholipids in a chloroform/methanol mixture (3:1, v/v). Peptides were dissolved in a DMSO/chloroform/methanol mixture (0.03:3:1, v/v/v). Lipid-peptide mixtures were prepared at the desired compositions and spread onto water, and then the solvent was allowed to evaporate for at least 10 min before compression was started, at a rate of 0.015 nm^2/molecule/min. For the subphase, unbuffered tridistilled water was used to create the same experimental conditions as those of the transfer.

AFM Observations. The topographies of the LB transferred monolayers were obtained using a Nanoscope IIIa Atomic Force Microscope from Veeco (DI, Santa Barbara, CA) working in the contact mode. Images were acquired under ambient conditions with a 120-μm piezoelectric scanner. Commercial silicon nitride cantilevers were used for measurements. The nominal imaging force during scanning was < 0.5nN (200-μm-long cantilever, $k = 0.120$ N/m). The scan rate was between 1 and 2.5 Hz. Images were obtained from at least two different samples prepared on different days with at least five macroscopically distinct areas on each sample.

RESULTS

Design of the Peptides. Peptides were designed based on the possibility that they would adopt different conformational states. The first was derived from the parent peptide (*22*, *23*) by a single W^7 to F^7 substitution generating the following sequence: G−A−L−F−L−G−F−L−G−A^{10}−A−G−S−T−M−G−A−W−S−Q^{20}−P−K−K−K−R−K−V. These peptides show the same conformational behavior as previously reported and the F^7 peptide, hereafter called peptide [Pβ], was shown to have a strong ability to deliver nucleic acids into cells in culture (*2*, *21*). This peptide is nonstructured in water but forms a sheet structure in the presence of phospholipids. Peptide [Pα], G−A−L−F−L−**A**−F−L−**A**−

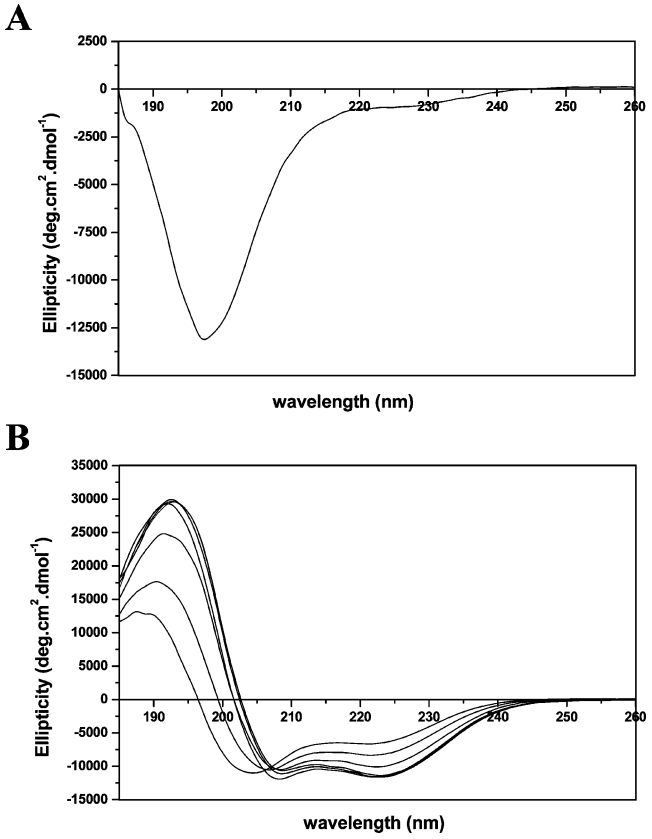

FIGURE 1: (A) Far UV CD spectrum of peptide [Pβ] in water. Addition of phosphate buffer does not induce any change in the spectrum and is therefore not shown. (B) Far UV CD spectrum of peptide [Pα] in water with increasing concentrations (0, 0.1, 0.2, 0.5, 1 and 2 M) phosphate buffer pH 7.2.

A^{10}−A−**L**−S−**L**−M−G−**L**−W−S−Q^{20}−P−K−K−K−R−K−V was designed as follows: based on the sequence of peptide [Pβ] and using the AGADIR algorithm (*26*), we selected a peptide with as much sequence similarity to peptide [Pβ] but which is predicted to have a greater helical content. The predicted helical content in the 1−16 region of peptide [Pα] is about 13% compared to 1% in peptide [Pβ].

Conformational Studies of the Analogues.

CD Investigations. When in solution in water, peptide [Pβ] exhibits a CD spectrum with a single minimum at 198 nm, characteristic of a nonordered structure (Figure 1A). The spectrum remains unchanged when the concentration of peptide is varied, and when either phosphate buffer or sodium chloride is added. For peptide [Pα], as expected from the predictive method, its CD spectrum with a maximum at 187 nm and a minimum at 205 nm associated with a shoulder around 220 nm is indicative of a tendency to adopt, at least in part, a helical conformation (*27*). This tendency is enforced by the addition of phosphate buffer or sodium chloride, which induces a slight shift of the extrema toward higher wavelength positions (194 and 207 nm) associated with a well-defined minimum at 222 nm, confirming the presence of an α-helical structure (Figure 1B).

For spectra obtained on transferred monolayers made of pure peptides, the spectrum of peptide [Pβ] strongly differs from that obtained when in solution in water. It is now characterized by a single minimum centered at 218 nm associated with a maximum at 191 nm (Figure 2, spectrum a). Such a spectrum is characteristic of a sheet structure. For peptide [Pα], the spectrum (Figure 2, spectrum b) displays a maximum at 190 nm and a minimum at 205 nm with a marked shoulder at 220 nm, which strongly resembles that observed in solution. It can, therefore, be stated that [Pα] remains in a helical conformation. In addition to identification of the conformational state, this spectrum provides a second piece of information that is related to the orientation of the helix with respect to the support plane. On the basis of the analysis reported by Wu et al. (*28*) on oriented α-helical polypeptides, the finding of a spectrum exhibiting the same characteristics as a classical spectrum of a helical structure, it can be stated that the helical axis is parallel to the plane of the support rather than perpendicular to the interface. Therefore, it is very likely that, when at the air−water interface, this axis is parallel to the interface.

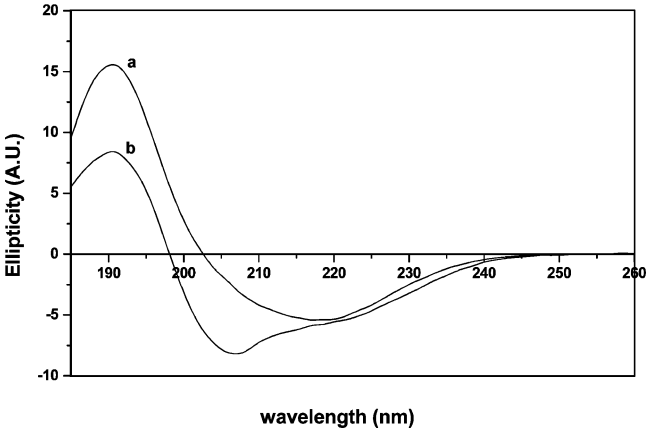

FIGURE 2: CD spectra of transferred monolayers of peptide [Pβ] (spectrum a) and peptide [Pα] (spectrum b).

FTIR Investigations in the Presence of Phospholipids. The influence of phospholipids on the conformation of the peptides was examined by FTIR. These experiments were carried out using the same procedure as reported previously (*29*). For peptide [Pβ], the FTIR spectra show that in the absence and in the presence of phospholipids (DOPC, DOPG, DPPC, and DPPG) at any peptide/lipid ratio, above 0.05, the sheet structure, as characterized by the presence of a major amide I band component centered around 1625 cm^{-1} is favored (Figure 3A). The existence of a broad contribution around 1650 cm^{-1} suggests the presence of unfolded domains as already observed by NMR studies of similar peptides engaged in micelles of SDS where the C-terminal NLS sequence always remains unfolded (*19*, *22*). It must be noted that neither the nature of the lipid nor the peptide/lipid ratio modify the conformational state of peptide [Pβ] as reported previously for a peptide containing the same hydrophobic sequence but with slight extensions at the C- and N-termini. For peptide [Pα], the α-helical structure is retained in all conditions as revealed by the presence of an amide I band at 1655 cm^{-1} without any detectable contribution at lower wavenumber (Figure 3B) (*30*).

Studies at the Air−Water Interface.

Adsorption. Lipid-Free Interface. Surface pressure measurements.

Figure 4 shows the surface pressure variations of the air−water interface induced by peptides [Pβ] and [Pα] injected into the subphase. Clearly, both peptides decrease the surface

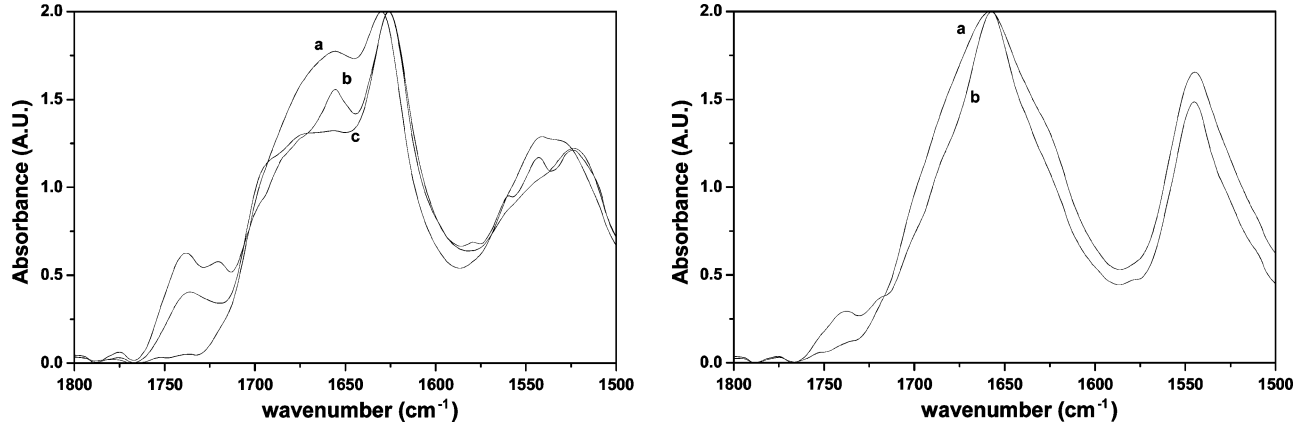

FIGURE 3: FTIR spectra of peptides [Pβ] (left panel) and [Pα] (right panel)Left panel: a, without phospholipid; b, in the presence of DOPG; c, in the presence of DOPC. Right panel: a, without phospholipid; b, in the presence of DOPC. Note that, in the presence of DOPC, the spectrum is superimposed with spectrum b and is therefore not shown.

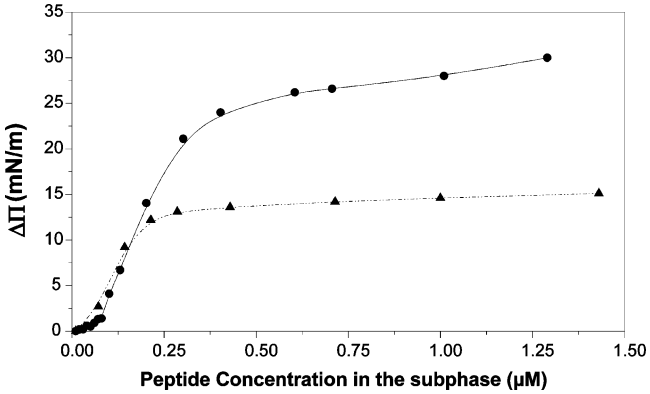

FIGURE 4: Peptide-induced variations of the surface pressures as a function of peptide concentrations in the subphase. ▲ Peptide [Pβ] ● Peptide [Pα].

tension of the air−water interface. However, although both peptides have very similar hydrophobic profiles based on their primary sequence, they induce different behaviors; the main difference is the greater decrease in tension induced by the helical peptide [Pα] than by [Pβ] (saturating pressures at 25 and 13 mN/m respectively). This suggests that peptide [Pα] develops stronger hydrophobic interactions than peptide [Pβ] when engaged in an air−water interface most likely because they adopt different structural states.

Lipid-Containing Interface. The ability of peptides [Pβ] and [Pα] to insert into phospholipid monolayers spread at the air−water interface was monitored by measuring variations in surface tension using different initial pressures, and by injecting a given peptide concentration in the subphase. The selected concentration is slightly less than the equilibrium spreading pressure of the peptide (*31*). Various penetration experiments were carried out using four different phospholipids where the nature of the headgroups (zwitterionic or negatively charged) and the physical state (liquid expanded or liquid condensed) were varied. The various plots of pressure variation versus the initial surface pressure are reported in Figure 5.

This figure reveals first that for peptide [Pα], when the lipid is in a liquid condensed state (LC), the nature of the headgroups has no influence on penetration, and the critical pressure of insertion obtained by extrapolation at initial pressure (Πi) = 0 of the variation of surface pressure ($\Delta\Pi$) induced by the peptide is high (37 mN/m) (Figure 5A and Table 1). In the case of peptide [Pβ], although still high (see Table 1), the critical pressure of insertion increases from 30 to 38 mN/m for DPPC and DPPG, respectively, indicating a better uptake by negatively charged phospholipids (Figure 5B and Table 1).

For lipids in the liquid expanded (LE) state, insertion depends on both the initial conformational state of the peptide and the nature of the headgroups. In all cases, the critical pressures of insertion are high (see Table 1 and Figure 5, parts C and D). Furthermore, the difference between the critical pressures of insertion occurring between negatively charged and neutral phospholipids is weak for the helical peptide (about 10 mN/m) compared to the other (about 17 mN/m) (compare Figure 5, parts C and D).

Further examination of Figure 5 also provides information on the interactions occurring between the two peptides and the phospholipids considered here. These are based on the pressure value measured for an air−water interface at low lipid content (i.e., at low initial pressure). The finding of surface pressures higher than these obtained for the pure peptides at saturation is indicative of strong peptide−lipid interactions (*32*). This is the case of [Pβ] particularly in the presence of negatively charged phospholipids and of [Pα] with DOPG.

Spreading at the Air−Water Interface. Compression Isotherms. Figure 6 shows the compression isotherms obtained for peptides [Pβ] and [Pα] when mixed with various phospholipids, DOPC, DOPG, DPPC and DPPG. The isotherms of the pure lipids are in agreement with those already reported (*33*−*35*). The isotherms were analyzed by examining the variation of the mean molecular area (that of the contributions of both the peptide and the lipid) as a function of the peptide/lipid ratio at a given and constant surface pressure. These variations are reported on the insets of Figure 6 and correspond to a pressure of 20 mN/m, which is below that of the collapse. Note that the same trends are observed at a pressure of 10 mN/m. Close examination of these insets indicates that, for all situations examined here, small but significant and reproducible deviations from linearity are observed and that several situations are encountered depending on the peptide−lipid combination. Interestingly, for lipids in the LE state, namely DOPC and DOPG, positive and negative deviations from linearity occur depending on the peptide conformation. The nonlinear variation of

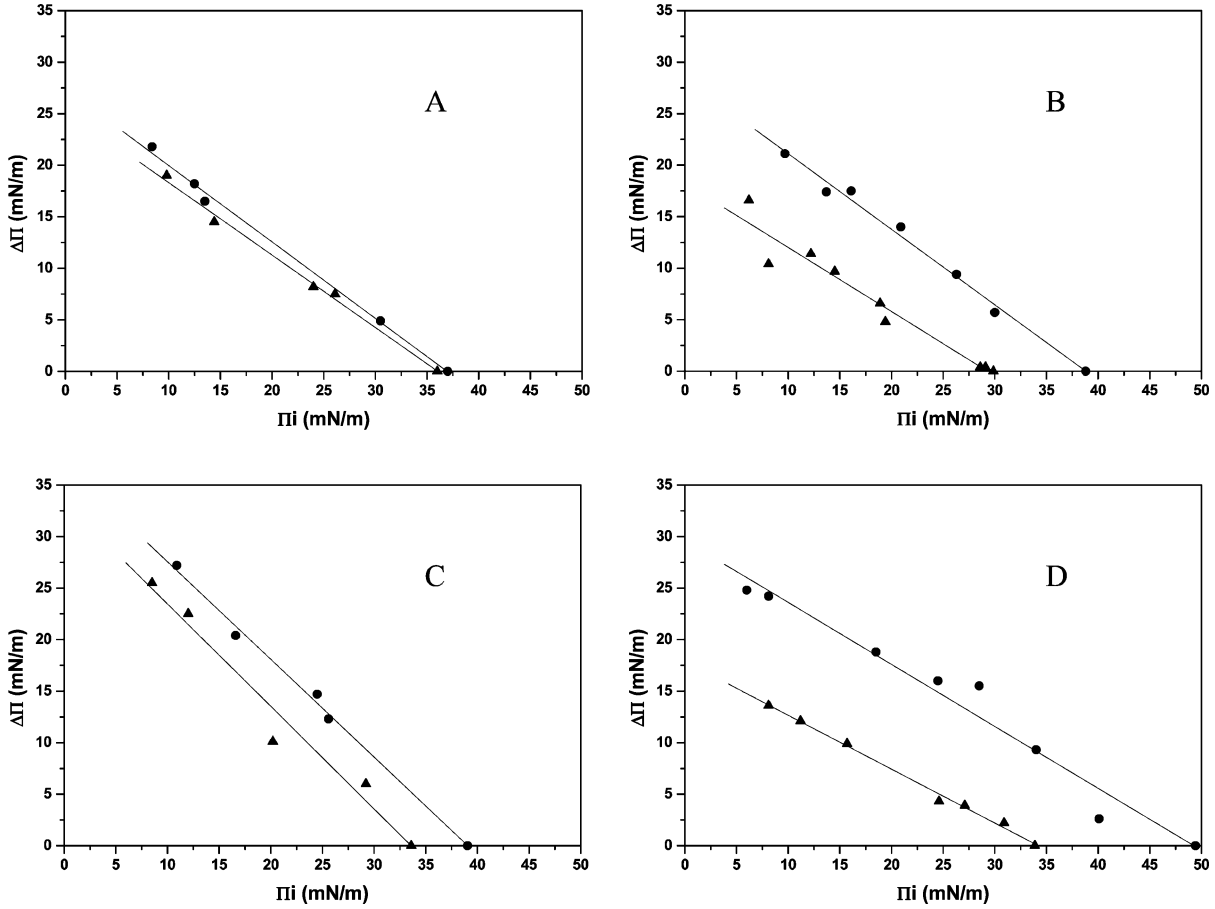

FIGURE 5: Surface pressure variations as a function of the initial pressure of the phospholipid monolayer. Peptide concentration in the subphase was 0.25 μM. (A) Peptide [Pα] in ▲ DPPC and in ● DPPG. (B) Peptide [Pβ] in ▲ DPPC and in ● DPPG. (C) Peptide [Pα] in ▲ DOPC and in ● DOPG. (D) Peptide [Pβ] in ▲ DOPC and in ● DOPG.

the mean molecular area provides a good argument suggesting that the peptides and lipids are miscible and interact (*36*−*38*). This further indicates that peptide [Pβ] interacts with DOPC and DOPG with contraction of the mean molecular area, while peptide [Pα] interacts with these phospholipids with an expansion of the mean molecular area. When investigating with phospholipids in the LC state (DPPC and DPPG), all peptide−lipid combinations reveal an expansion of the mean molecular area, indicating that the peptides interact with and are miscible with DPPC and DPPG.

AFM Observations. AFM observations were performed in air on LB films transferred at a surface pressure of 26 mN/m onto a cleaved mica surface. Accordingly, the AFM tip imaged the hydrophobic side of the monolayer. As compared to pure DOPC films, the roughness of peptide [Pα]-containing DOPC monolayers (x_{pep}= 0.15) was significantly increased (mean roughness 0.089 nm vs 0.060 nm, Figure 7A). This also applied to peptide [Pα]-containing DOPG films (mean roughness 0.097 nm, Figure 7B). This roughness corresponded to the presence of round-shaped structures 15−25 nm in diameter. As in the films made of pure [Pα] peptide filamentous structures ∼15 nm in diameter, up to 1 μm in length and protruding by ∼0.5nm (Figure 8A) were also present in [Pα]/DOPC monolayers. However, they were not detected in [Pα]/DOPG films. Addition of [Pα] to the solution spread at the air/water interface had a marked effect for films made of saturated phospholipid species DPPC (Figure 7C) and DPPG (Figure 7D). Thus, instead of a flat surface, with perhaps a few linear defects (*39*, *40*), AFM imaging revealed a complex topography with light domains, corresponding to DPPC liquid condensed phase surrounded by a darker matrix, ∼1.1 nm thinner. The size of the LC domains varies from a couple to a few hundred nanometers. Some filaments decorated the darker matrix (arrows). The structure of the DPPG films was also disorganized with the presence of both large and small smooth LC domains surrounded by a darker matrix, enriched in peptide. As for DPPC, the lighter domains protruded by ∼1.1 nm from the darker matrix. On the other hand, no filaments could be visualized in [Pα]/DPPG monolayers. This disruption of gel phase organization induced by the peptide strongly suggests the existence of hydrophobic interactions between [Pα] and the phospholipids. In addition, the absence of filaments for PG species also suggests that the negatively charged PG polar headgroups enhance the lipid−peptide interactions at the expense of peptide−peptide interactions.

The imaged obtained with [Pβ] and phosphatidylcholine phospholipids were comparable to those obtained with [Pα] with the presence of both filaments and small aggregates in DOPC films and an important reduction of the DPPC gel phase domains associated with the appearance of filaments in the darker matrix (Figure 9, parts A and C). The presence of filaments in these samples was unexpected because pure [Pβ] formed globular aggregates, 20 nm in section, but no filaments (Figure 8). The results of experiments performed with DOPG and DPPG revealed a behavior that markedly differed from that of [Pα]. First, in DOPG (Figure 9B) the size of peptide-induced structures significantly increased, up

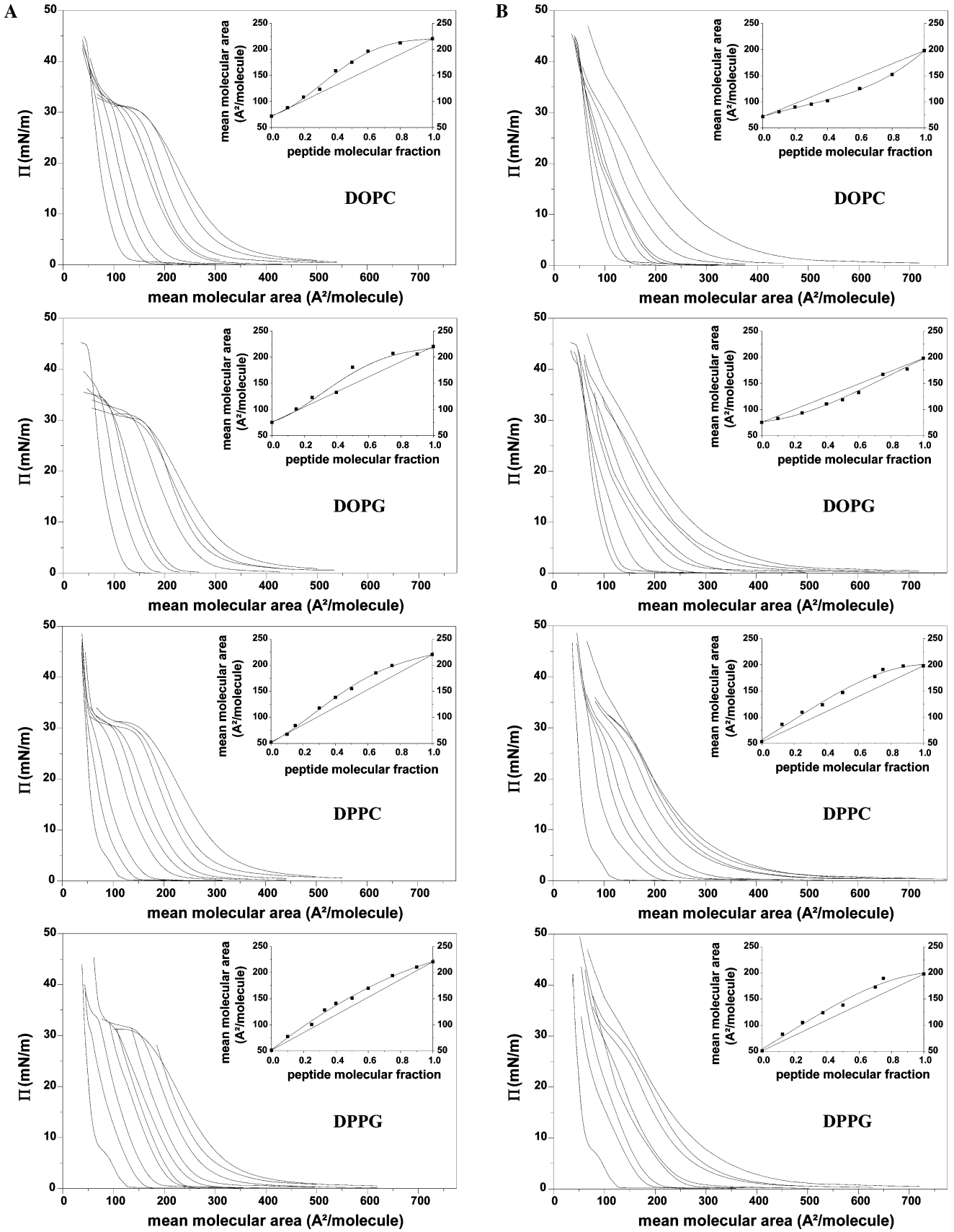

FIGURE 6: Compression isotherms of peptides [Pα] (A) and [Pβ] (B) in the presence of various phospholipids and at various peptide/lipid ratios. The insets show the variations of the mean molecular areas as a function of peptide/lipid ratios.

to ~50 nm for individual globular structures. Furthermore, larger domains of various shapes, likely resulting from the coalescence of individual globular structures are also formed (arrows). Gel phase DPPG domains can no longer be identified in [Pβ]-DPPG films that appeared to be constituted of aggregates of different sizes and thicknesses (Figure 9D).

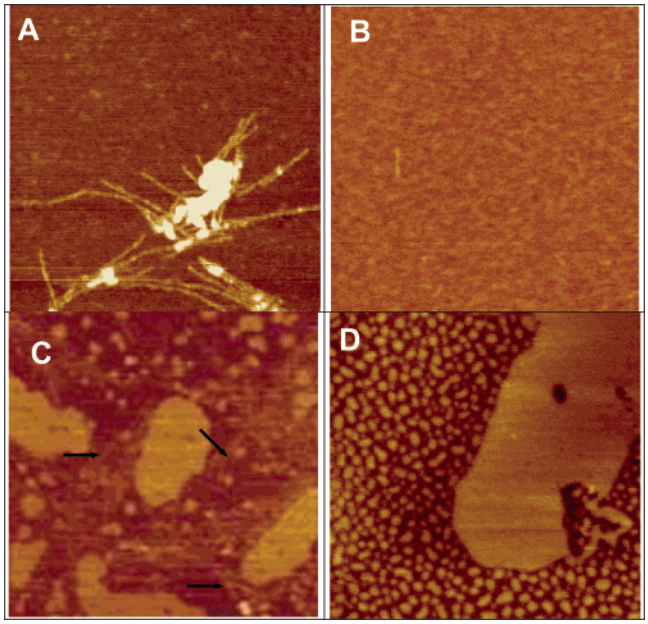

FIGURE 7: AFM imaging of LB monolayers composed of [Pα] and DOPC (A), DOPG (B), DPPC (C), and DPPG (D) at a molar ratio of $x_{[5]} = 0.15$. The scan size is 1 μm × 1 μm, and the *z* scale is 3 nm for A, B and D; 5 nm for C.

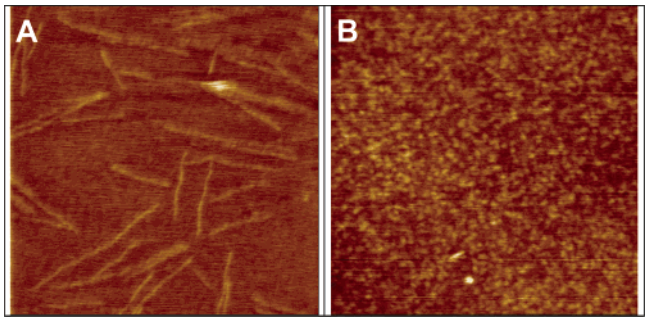

FIGURE 8: AFM imaging of LB monolayers composed of pure [Pα] (A) and pure [Pβ] (B). The scan size is 1 μm × 1 μm, and the *z* scale is 3 nm.

This drastic reorganization of monolayers likely results from the strongest interactions between [Pβ] and the negatively charged phospholipids.

DISCUSSION

The present investigations point out that the conformational properties of primary amphipathic carrier peptides with similar primary sequences can influence their interactions with phospholipids and subsequently their cellular uptake through the membrane.

Membrane uptake is dependent on the conformational state. Two starting states have to be considered (i.e., those adopted when the peptides are in solution in water or in buffer). The first one corresponds to a peptide that is in a nonordered state, as occurs for [Pβ]. Upon its uptake at an interface containing phospholipids or not, this peptide undergoes a conformational transition into a sheet type structure. The second situation is exemplified by peptide [Pα], which always adopts a helical conformation. By analogy with previous studies carried out on peptides of the same family, the helical moiety spans the hydrophobic domain, while the hydrophilic NLS domain is nonstructured. Considering the consequences of these conformational differences on uptake, it appears clear that for helical peptide [Pα], the nature of the phospholipid headgroups has no (LC) or little (LE) effect, while peptide [Pβ] exhibits a better penetration ability in negatively charged DOPG than in the neutral DOPC. It also appears that both peptides interact with all phospholipids, as shown by analysis of the compression isotherms. Finally, it must also be noted that all critical pressures of insertion are higher than 30 mN/m, suggesting that peptides [Pβ] and [Pα] can spontaneously insert into phospholipid bilayers (*41*).

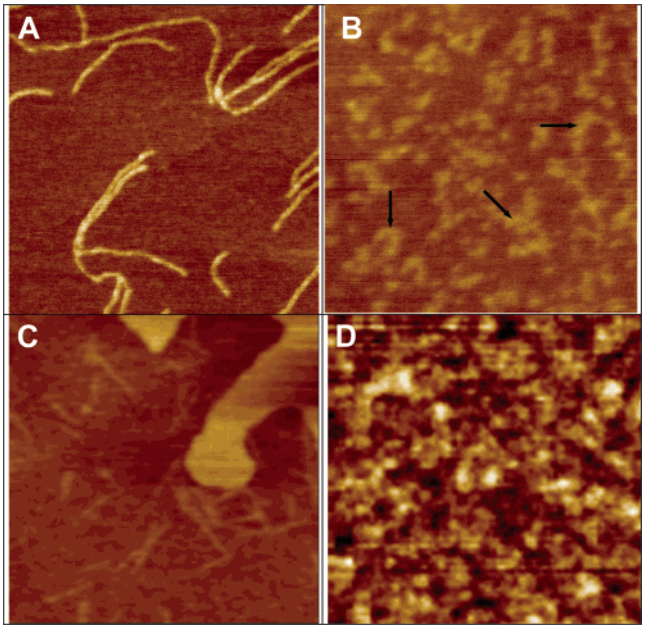

FIGURE 9: AFM imaging of LB monolayers composed of [Pβ] and DOPC (A), DOPG (B), DPPC (C) and DPPG (D) at a molar ratio of $x_{[5]} = 0.15$. The scan size is 1 μm × 1 μm, and the *z* scale is 3 nm.

Analysis of the compression isotherms through examination of the variations of mean molecular areas versus molecular ratios reveals a nonlinear behavior for all peptide−phospholipid mixtures, indicating that both peptides are miscible and interact with all the phospholipids used in the present work. Clearly, several situations occur, because positive and negative deviations are observed. For the phospholipids in the LC state, a positive deviation is observed irrespective of the peptide type, suggesting that the peptides interact with the lipids through repulsive interactions. However, the AFM observations showed that the presence of peptide disrupted the lipid organization. Therefore, at this stage, we cannot decide whether the expansion of the mean molecular area reflects only the peptide-lipid interactions or the modification of the physical sate of the lipids or both.

In the presence of lipids in the LE state, contraction and expansion occurs for peptides [Pβ] and [Pα], respectively. The contraction observed in the case of [Pβ] indicates that the peptide−lipid interactions are attractive and may reflect the formation of peptide−lipid complexes through hydrophobic interactions, as already detected by mass spectrometry (*42*). For peptide [Pα], the origin of the expansion is not very clear because it also forms complexes with phospholipids, which would suggest a behavior similar to that of [Pβ]. Because no lipid-induced conformational change of the peptide was detected as was found for the SP−NLS peptide, it is possible that the expansion reflects a change in the

orientation of the peptide with respect to the air−water interface, from a position parallel to interface in the absence of lipid to a more vertical position in the presence of lipid in order to satisfy the hydrophobic peptide−lipid interactions.

All these conclusions are supported by the AFM observations, which clearly indicate the existence of peptide−lipid interactions, because phospholipids modify the shape and size of the peptide-containing particles formed in the absence of phospholipids and vice versa; the presence of the peptides disrupts the lipid organization.

Possible Consequences on the Cellular Uptake of Nucleic Acids. Conformational investigations indicate that peptide [Pα] is helical, and thus most of the peptide bonds of the hydrophobic domain are engaged in hydrogen bonds. According to Wimley and White (*43*), such a situation is favorable for membrane insertion through the hydrophobic domain. For peptide [Pβ], which is nonordered in water, insertion into a lipidic medium in this form is impossible for energetic reasons (*44*). Insertion requires formation of a hydrogen bonding pattern leading to a β-sheet structure. When the hydrogen bonds are established, the peptides can penetrate into the lipidic core and the peptide-lipid hydrophobic interactions may participate in the translocation process. Since all data indicate that both peptides can penetrate into phospholipid bilayers and that they strongly interact with the phospholipids through hydrophobic interactions, one would expect that both peptides would exhibit the same or similar vectorization properties. Preliminary assays, however, reveal that although both peptides can form complexes with siRNAs, only those taken up by cells and mediated by peptide [Pβ] (or its K to S analogue) enabled siRNA-induced activities (*45*). This observation stresses the influence of the conformation of the carrier peptide on the transfer and induced activity of a nucleic acid. Does the helical conformation enhance the stability of the complex and thus would it reduce the siRNA decaging process, or is the conformation responsible for a modification of the final cellular localization of the complex? Further investigations are currently in progress to identify precisely the origin of this difference.

In conclusion, conformational investigations of cell penetrating peptides in the presence or absence of phospholipids, associated with studies of peptide−lipid interactions by the monolayer approach, point out that the conformational state of a peptide can influence its uptake by model membranes. While no or nearly no selectivity for headgroups can be detected for the helical peptide, the other peptide shows a marked preference to penetrate into negatively charged phospholipids. Finally, the presence of peptide can strongly disrupt the organization of the membrane, as revealed by atomic force microscopy imaging.

ACKNOWLEDGMENT

Our thanks are due to Dr. M. C. Morris for helpful discussions and help in correcting the manuscript and to Dr. N. Van Mau for her skilful advice.

REFERENCES

1. Mahato, R. I. (1997) Nonviral peptide-based approaches to gene delivery. *J. Drug Targeting 7*, 249−268.
2. Morris, M. C., Chaloin, L., Heitz, F., and Divita, G. (2000) Translocating peptides and proteins and their use for gene delivery. *Curr. Opin. Biotechnol. 11*, 461−466.
3. Gariépy, J., and Kawamura, K. (2001) Vectorial delivery of macromolecules into cells using peptide-based vehicles. *Trends Biotechnol. 19*, 21−28.
4. Rittner, K., Benavente, A., Bompard-Sorlet, A., Heitz, F., Divita, G., Brasseur, R., and Jacobs, E. (2002) New basic membrane-destabilizing peptides for plasmid-based gene delivery in vitro and in vivo. *Mol. Ther. 5*, 104−114.
5. Wadia, J. S., and Dowdy, S. F. (2002) Protein transduction technology. *Curr. Opin. Biotechnol. 13*, 52−56.
6. Dom, G., Show-Jackson, C., Matis, C., Bouffioux, O., Picard, J. J., Prochiantz, A., Mingeot-Leclercq, M. P., Brasseur, R., and Rezsohazy, R. (2003) Cellular uptake of Antennapedia Penetratin peptides is a two-step process in which phase transfer precedes a tryptophan-dependent translocation. *Nucleic Acids Res. 31*, 556−561.
7. Schwarze, S. R., Ho, A., Vocero-Akbani, A., ans Dowdy, S. F. (1999) In vivo protein transduction: delivery of a biologically active protein into the mouse. *Science 285*, 1569−1572.
8. Dathe, M., and Wieprecht, T. (1999) Structural features of helical antimicrobial peptides: their potential to modulate activity on model membranes and biological cells. *Biochim. Biophys. Acta 1462*, 71−87.
9. Oehlke, J., Scheller, A., Wiesner, B., Krause, E., Beyermann, M., Klauschenz, E., Melzig, M., and Bienert, M. (1998) Cellular uptake of an α-helical amphipathic model peptide with the potential to deliver polar compounds into the cell interior nonendocytically. *Biochim. Biophys. Acta 1414*, 127−139.
10. Vivès, E., Brodin, P., and Lebleu, B. (1997) A truncated HIV-1 Tat protein basic domain rapidly translocates through the plasma membrane and accumulates in the cell nucleus. *J. Biol. Chem. 272*, 16010−16017.
11. Wyman, T. B., Nicol, F., Zelphati, O., Scaria, P. V., Plank, C., and Szoka, F. C., Jr. (1997) Design, synthesis, and characterization of a cationic peptide that binds to nucleic acids and permeabilizes bilayers. *Biochemistry 36*, 3008−3017.
12. Lindgren, M., Gallet, X., Soomets, U., Hallbrink, M., Brakenhielm, E., Pooga, M., Brasseur, R., and Langel, Ü. (2000) Translocation properties of novel cell penetrating transportan and penetratin analogues. *Bioconjug. Chem. 11*, 619−626.
13. Rudolph, C., Plank, C., Lausier, J., Schillinger, U., Muller, R. H., and Rosenecker, J. (2003) Oligomers of the arginine-rich motif of the HIV-1 TAT protein are capable of transferring plasmid DNA into cells. *J Biol Chem. 278*, 11411−11418.
14. Leonetti, J. P., Degols, G., and Lebleu, B. (1990) Biological activity of oligonucleotide-poly(L-lysine) conjugates: mechanism of cell uptake. *Bioconjug. Chem. 1*, 149−153.
15. Futaki, S., Suzuki, T., Ohashi, W., Yagami, T., Tanaka, S., Ueda, K., and Sigiura, Y. (2001) Arginine-rich peptides. An abundant source of membrane-permeable peptides having potential as carriers for intracellular protein delivery. *J. Biol. Chem. 276*, 5836−5840.
16. Briggs, M. S., and Gierasch, L. M. (1986) Molecular mechanisms of protein secretion: the role of the signal sequence. *Adv. Protein Chem. 38*, 109−180.
17. Slepushkin, V. A., Andreev, S. M., Sidorova, M. V., Melikyan, G. B., Grigoriev, V. B., Chumakov, V. M., Grinfeldt, A. E., Manukyan, R. A., and Karamov, E. V. (1992) Investigation of human immunodeficiency virus fusion peptides. Analysis of interrelations between their structure and function. *AIDS Res. Hum. Retroviruses 8*, 9−18.
18. Goldfarb, D. S., Gariépy, J., Schoolnik, G., and Kornberg, R. D. (1986) Synthetic peptides as nuclear localization signals. *Nature 322*, 641−644.
19. Chaloin, L., Vidal, P., Heitz, A., Van Mau, N., Méry, J., Divita, G., and Heitz, F. (1997) Conformations of Primary Amphipathic Carrier Peptides in Membrane Mimicking Environments. *Biochemistry 36*, 11179−11187.
20. Chaloin, L., Vidal, P., Lory, P., Méry, J., Lautredou, N., Divita, G., and Heitz, F. (1998) Design of Carrier Peptide−Oligonucleotide Conjugate with Rapid Membrane Translocation and Nuclear Localization Properties. *Biochim. Biophys. Res. Commun. 243*, 601−608
21. Morris, M. C., Vidal, P., Chaloin, L., Heitz, F., and Divita, G. (1997) A new peptide vector for efficient delivery of oligonucleotide into nontransformed mammalian cells. *Nucleic Acid Res. 25*, 2730−2736.
22. Vidal, P., Chaloin, L., Heitz, A., Van Mau, N., Méry, J., Divita, G., and Heitz; F. (1998) Conformational Analysis of Primary

Amphipathic Carrier Peptides and Origin of the Various Cellular Localizations. *J. Membr. Biol. 162*, 259−264.
23. Vidal, P., Chaloin, L., Méry, J., Lamb, N., Lautredou, N., Bennes, R., and Heitz, F. (1996) Solid-phase Synthesis and Cellular Localization of a C- and/or N-terminal Labeled Peptide. *J. Pept. Sci. 2*, 125−133.
24. Briggs, M. S., Cornell, D. G., Dluhy, R. A., and Gierasch, L. M. (1986) Conformations of signal peptides induced by lipids suggest initial steps in protein export. *Science 233*, 206−208.
25. Van Mau, N., Vié, V., Chaloin, L., Lesniewska, E., Heitz, F., and Le Grimellec, C. (1999) Lipid-Induced Organization of a Primary Amphipathic Peptide. A coupled AFM-Monolayer Study. *J. Membr. Biol. 167*, 241−249.
26. Munoz, V., and Serrano, L. (1997) Development of the multiple sequence approximation within the AGADIR model of alpha-helix formation: comparison with Zimm-Bragg and Lifson-Roig formalism. *Biopolymers 41*, 495−509.
27. Greenfield, N., and Fasman, G. D. (1969) Computed circular dichroism spectra for the evaluation of protein conformation. *Biochemistry 8*, 4108−4116.
28. Wu, Y., Huang, H. W., and Olah, G. A. (1990) Method of oriented circular dichroism. *Biophys. J. 57*, 797−806.
29. Vié, V., Van Mau, N., Chaloin, L., Lesniewska, E., Le Grimellec, C., and Heitz, F. (2000) Detection of Peptide − Lipid Interactions in Mixed Monolayers, Using Isotherms, Atomic Force Microscopy, and Fourier Transform Infrared Analyses. *Biophys. J. 78*, 846−856.
30. Arrondo, J. L., Muga, A., Castreana, J., and Goni, F. M. (1993) Quantitative studies of the structure of proteins in solution by Fourier transform infrared spectroscopy. *Prog. Biophys. Mol. Biol. 59*, 23−56.
31. Rafalski, M., Lear, J. D., and DeGrado, W. F. (1990) Phospholipid interactions of synthetic peptides representing the N-terminus of HIV gp41. *Biochemistry 29*, 7917−7922.
32. Maget-Dana, R. (1999) The monolayer technique: a potent tool for studying the interfacial properties of antimicrobial and membrane-lytic peptides and their interactions with lipid membranes. *Biochim. Biophys. Acta 1462*, 109−140.
33. Lakhdar-Ghazal, F., and Tocanne, J. F. (1981) Phase behaviour in monolayer and in water dispersions of mixtures of dimannosyldiacylglycerol with phosphatidylglycerol. *Biochim. Biophys. Acta 644*, 284−294.
34. Tamm, L. K., and McConnell, H. M. (1985) Supported phospholipid bilayers. *Biophys. J. 47*, 105−113.
35. Ruano, M. L., Nag, K., Worthman, L.-A., Casals, C., Pérez-Gil, J., and Keough, K. M. W. (1998) Differential partitioning of pulmonary surfactant protein SP-A into regions of monolayers of dipalmitoylphosphatidylcholine and dipalmitoylphosphatidylcholine/dipalmitoylphosphatidylglycerol. *Biophys. J. 74*, 1101−1109.
36. Crisp, D. J. (1949) A two-dimensional phase rule. I. Derivation of a two-dimensional phase rule for planar interface. II. Some applications of a two-dimensional phase rule for a single surface. In *Surface Chemistry* Butterworths, London, 17−35.
37. Gaines, G. L. (1966) Mixed monolayers. In *Insoluble Monolayers at Liquid−Gas Interfaces.* Prigogine, Ed. Interscience, New York, 281−300.
38. Taneva, S., and Keough, K. M. W. (1994) Pulmonary surfactant proteins SP-B and SP-C in spread monolayers at the air−water interface. I. Monolayers of pulmonary surfactant protein SP-B and phospholipids. *Biophys. J. 66*, 1137−1148.
39. Vié, V., Van Mau, N., Lesniewska, E., Goudonnet, J. P., Heitz, F., and Le Grimellec, C. (1998) Distribution of Ganglioside GM1 between Two-component, Two-phase Phosphatidylcholine Monolayers. *Langmuir 14*, 4574−4593.
40. Yuan, C., and Johnston, L. J. (2000) Distribution of ganglioside GM1 in L-α-dipalmitoylphosphatidylcholine/cholesterol monolayers: a model for lipid rafts. *Biophys. J. 79*, 2768−2781.
41. Demel, R. A., Geurts van Kessel, W. S., Zwaal, R. F., Roelofsen, B., and van Deenen, L. L., (1975) Relation between various phospholipase actions on human red cell membranes and the interfacial phospholipid pressure in monolayers. *Biochim. Biophys. Acta 406*, 97−107.
42. Li, Y., Heitz, F., Le Grimellec, C., and Cole, R. B., (2004) Hydrophobic component in noncovalent binding of fusion peptides to lipids as observed by electrospray mass spectrometry. *Rapid Commun. Mass Spectrom. 18*, 135−137.
43. Wimley, W. C., and White, S. H., (2000) Designing transmembrane α-helices that insert spontaneously. *Biochemistry 39*, 4432−4442.
44. White, S. H., and Wimley, W. C., (1999) Membrane protein folding and stability: physical principles. *Annu. Rev. Biophys. Biomol. Struct. 28*, 319−365.
45. Deshayes, S., Van Mau, N., Morris, M. C., Divita, G., and Heitz, F., (2004) Structural requirements for noncovalent peptide-mediated cellular delivery of siRNAs. Proceedings of the 18th American Peptide Symposium (in press).

BI049298M